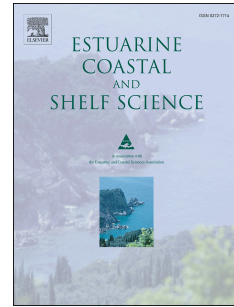


# Journal Pre-proof

Integrated use of otolith shape and microchemistry to assess *Genidens barbatus* fish stock structure

Thaís Rodrigues Maciel, Marcelo Vianna, Barbara Maichak de Carvalho, Nathan Miller, Esteban Avigliano



PII: S0272-7714(21)00410-8

DOI: <https://doi.org/10.1016/j.ecss.2021.107560>

Reference: YECSS 107560

To appear in: *Estuarine, Coastal and Shelf Science*

Received Date: 16 June 2021

Revised Date: 27 July 2021

Accepted Date: 15 August 2021

Please cite this article as: Maciel, Thaís.Rodrigues., Vianna, M., Maichak de Carvalho, B., Miller, N., Avigliano, E., Integrated use of otolith shape and microchemistry to assess *Genidens barbatus* fish stock structure, *Estuarine, Coastal and Shelf Science* (2021), doi: <https://doi.org/10.1016/j.ecss.2021.107560>.

This is a PDF file of an article that has undergone enhancements after acceptance, such as the addition of a cover page and metadata, and formatting for readability, but it is not yet the definitive version of record. This version will undergo additional copyediting, typesetting and review before it is published in its final form, but we are providing this version to give early visibility of the article. Please note that, during the production process, errors may be discovered which could affect the content, and all legal disclaimers that apply to the journal pertain.

© 2021 Published by Elsevier Ltd.

1 **Integrated use of otolith shape and microchemistry to assess *Genidens barb* fish**  
2 **stock structure**

3

4 Thaís Rodrigues Maciel<sup>a</sup>, Marcelo Vianna<sup>a,b</sup>, Barbara Maichak de Carvalho<sup>c</sup>, Nathan  
5 Miller<sup>d</sup>, Esteban Avigliano<sup>e</sup> \*

6

7 <sup>a</sup> Instituto de Biologia, Universidade Federal do Rio de Janeiro, Av. Carlos Chagas  
8 Filho, 373, Ilha do Fundão, (21941-541) Rio de Janeiro, RJ, Brazil.

9 <sup>b</sup> Instituto Museu Aquário Marinho do Rio de Janeiro-AquaRio (IMAM/AquaRio) – Rio  
10 de Janeiro Marine Aquarium Research Center, Rio de Janeiro, Brazil. E-mail address:  
11 mvianna@biologia.ufrj.br

12 <sup>c</sup> Programa de Pós-Graduação em Engenharia Ambiental, Departamento de Engenharia -  
13 Universidade Federal do Paraná, Centro Politécnico, (81531-970) Bairro Jardim das  
14 Américas, Curitiba, Paraná, Brazil. E-mail address: bmaicarvalho@gmail.com

15 <sup>d</sup> Jackson School of Geosciences, University of Texas at Austin, Austin, (78712) Texas,  
16 USA. E-mail address: nrmiller@jsg.utexas.edu

17 <sup>e</sup> Instituto de Investigaciones en Producción Animal (INPA-CONICET-UBA), Facultad  
18 de Ciencias Veterinarias, Universidad de Buenos Aires (UBA), Av. Chorroarín 280,  
19 (C1427CWO) Ciudad Autónoma de Buenos Aires, Argentina. E-mail address:  
20 estebanavigliano@conicet.gov.ar

21 \* Corresponding author: estebanavigliano@conicet.gov.ar

22

23

24

25

26 **Abstract**

27 Otolith composition (edge vs core: Mg/Ca, Mn/Ca, Zn/Ca, Sr/Ca, Ba/Ca) by LA-ICP-  
28 MS and Elliptic Fourier analysis were integrated to evaluate spatial segregation of adult  
29 and juvenile stages of *Genidens barbatus* from specimens collected from five coastal  
30 areas off Brazil (Paraíba do Sul River, Guanabara Bay, Itapanhaú River mouth,  
31 Paranaguá Bay), Argentina and Uruguay (La Plata Estuary). Fisheries of this  
32 diadromous catfish have largely collapsed in the southwest Atlantic coastal region due  
33 to overexploitation. An understanding of population structure is now critically needed  
34 for improved management strategies for this endangered species. PERMANOVA based  
35 on chemistry showed significant differences ( $p < 0.05$ ) between all sites, except  
36 Itapanhaú River and Paranaguá Bay (edge). Shape, by comparison, found significant  
37 differences between all sampling sites, except Guanabara Bay and Paranaguá Bay, and  
38 Itapanhaú River and Paranaguá Bay. Discriminant analysis cross-classification success  
39 based on chemistry ranged from 33.3 (Paranaguá Bay) to 100% (La Plata Estuary), and  
40 66.7 (Paranaguá Bay) to 100% (La Plata Estuary) for otolith edges (mean=61.3%) and  
41 cores (mean=78.9%). For otolith shape, the jackknifed rate (mean=45.9%) was  
42 relatively low for all sites (32.1-44.7%) except La Plata Estuary (67.6%). Although we  
43 do not find otolith shape to be particularly useful; otolith microchemistry supports the  
44 presence of different management units. The results revealed that on a small geographic  
45 scale (~300 km) microchemistry might not be efficient to discriminate between some  
46 sampling sites.

47

48 **Key words:** catfish; estuaries; fish stock; segregation; trace elements.

49

50

51

52

53

54

55

## 56 **1. Introduction**

57 The diadromous catfish *Genidens barbatus* (Lacépède 1803), family Ariidae, inhabits  
58 freshwater, estuarine and marine environments ranging from Bahía (Brazil) to Patagonia  
59 (Argentina) (Caille et al., 1995; López and Bellisio, 1965). This catfish presents a  
60 plastic and complex life cycle, including differing amphidrome migration patterns and  
61 resident freshwater specimens (Avigliano et al., 2021, 2017c, 2015b). Amphidromus  
62 specimens typically migrate from the sea/estuary to lower salinity waters during  
63 reproduction period (Avigliano et al., 2017c). Males perform oral incubation of  
64 offspring, releasing them in the mouth of the estuary, where they remain until complete  
65 development, and then migrate as far as the continental platform (Avigliano et al.,  
66 2017c, 2015b, 2015c; Reis, 1986a).

67 Formerly an important species for artisanal fishing, mainly in Southern Brazil (Gomes  
68 and Araújo, 2004; Reis, 1986b; Velasco et al., 2007), the catch rate has dropped  
69 significantly in recent decades. In response to dramatic declines in landings (e.g., from  
70 30,000 in 1962 to 10,000 in 2011; (Mendonça et al., 2017), *G. barbatus* was added to  
71 the List of Endangered Brazilian Fauna, subsequently banning its capture, transport, and  
72 storage (MMA, 2014). Factors besides overfishing, such as pollution and habitat loss,  
73 also contribute to this decline (Barletta and Lima, 2019; Kime, 1995). Complex  
74 reproduction and high age of first maturity (8.5 years for females and 9 years for males,  
75 (Reis, 1986a) also hinder the recovery of this fishery species. Thus, effective  
76 management of *G. barbatus* stocks is essential to their recovery. The term “fishing stock”  
77 refers to a commercially exploited resource that is included within fishery management  
78 strategies (Begg and Waldman, 1999). Fishing stocks are basic work units in which the  
79 state of fisheries is assessed and management policies applied to implement sustainable  
80 exploitation (Tanner, et al., 2015). Among the various techniques available for

81 identifying fish stocks, chemical fingerprinting of calcified structures, such as otoliths,  
82 has proven to be one of the most efficient. Otoliths are calcified structures present in the  
83 inner ear of teleost fish that form by continuous outward (radial) growth through life  
84 (Campana, 1999). Ambient water is the predominant source of most inorganic elements  
85 deposited in its matrix (Campana, 1999; Hüseyin et al., 2020; Kerr and Campana, 2014),  
86 although diet, ontogeny and genetics can also affect its chemical composition (Clarke et  
87 al., 2011; Elsdon, and Gillanders, 2003; Morales-Nin, 2000). Because otoliths are  
88 metabolically inert structures, the elements deposited in their accreting surface layers  
89 are permanently retained (Campana, 1999), and the core-to-edge chemical composition  
90 can be used as a biological tracer to discriminate between fish groups that spend parts of  
91 their lives in different areas (Kerr and Campana, 2014). In fact, otolith core and edge  
92 elemental signatures have proven useful for identifying both nursery areas (Avigliano et  
93 al., 2016; Bailey et al., 2015; Patterson et al., 2008) and discriminating fish stocks  
94 (Avigliano, 2021; Kerr and Campana, 2014; Soeth et al., 2019; Tanner, et al., 2015).

95 In Southwestern Atlantic (South America) coastal waters, a relationship between the  
96 water and *G. barbatus* otoliths has been reported for Ba:Ca and Mn:Ca ratios (Avigliano  
97 et al., 2019). Other microchemical studies have identified four *G. barbatus* nursery areas  
98 using otolith core compositions (Avigliano et al., 2016) and five fish stocks through  
99 integration of dorsal fin spine and otolith edge compositions (Avigliano, et al., 2017;  
100 Avigliano et al., 2019). However, evidence supporting the existence of different stocks  
101 is fragmented because the studies have thus far been limited to widely separated  
102 geographic areas (e.g., 700-1000 km spacing) and have sampled limited portions of life  
103 histories (e.g., otolith edges). Critically needed are studies integrating sampling sites  
104 with differing spacings but covering the entire distribution area of this fishery.

105 Besides the life history information gained from otolith chemistry, otolith shape can  
106 provide complementary marker information for stock discrimination (Biolé et al., 2019;  
107 Hüsey et al., 2016; Ibáñez et al., 2017). Genetic and environmental factors (*e.g.*  
108 temperature, depth, salinity and food availability) can significantly impact fish growth  
109 rates and otolith growth patterns (Longmore, et al., 2010; Vignon and Morat, 2010a).  
110 Accordingly, fish that experience different environmental conditions may tend to  
111 present differences in otolith shape, and these differences can be statistically  
112 characterized. Otolith shape (morphometry) analysis is also much more economical than  
113 microchemistry and has proven useful for discerning habitat use (Avigliano et al.,  
114 2015d, 2014), sexual dimorphism (Maciel et al., 2019), species (Avigliano et al., 2018;  
115 Gut et al., 2020), relative growth (Maciel et al., 2019; Perin and Vaz-dos-Santos, 2014),  
116 stocks (Annabi et al., 2013; Biolé et al., 2019; Soeth et al., 2019) and nursery areas  
117 (Avigliano et al., 2017b). More efficient and accurate stock characterization may thus  
118 be obtained from integrated studies of otolith morphometry and chemistry (Biolé et al.,  
119 2019; Longmore, et al., 2010; Soeth et al., 2019).

120 Toward improved management strategies of this endangered species, we integrate  
121 otolith microchemistry and morphometry to discern *G. barbatus* population structure in  
122 the main area of its distribution in the Southwestern Atlantic coastal region.

123

## 124 **2. Materials and methods**

### 125 **2.1. Study area**

126 *Genidens barbatus* specimens were collected from five Southwestern Atlantic coastal  
127 river mouth estuaries, four off Brazil: 1) Paraíba do Sul River, 2) Guanabara Bay, 3)  
128 Itapanhaú River, 4) Paranaguá Bay, and one off Argentina-Uruguay: 5) La Plata (Figure  
129 1).

130 Paraíba do Sul River mouth is a delta (Krüger et al., 2006) located in Rio de Janeiro  
131 state (21°36'23.9"S, 41°02'43.8"W), near the frontier with Espírito Santo state (Brazil).  
132 The delta is characterized by beach ridges, that separate a main estuary in the Altafona  
133 region from a secondary estuary in the Gargaú region (Bernini and Rezende, 2004).  
134 Paraíba do Sul River has a length of 1145 km, a drainage basin of 55.400 km<sup>2</sup> and  
135 salinities ranging from 0 to 30‰ (Krüger et al., 2006). Guanabara Bay, southeast of Rio  
136 de Janeiro State (Brazil) (22°48'24.3"S, 43°09'14.7"W), is a semi-closed estuarine  
137 coastal ecosystem (Meniconi et al., 2012). It has an area of 380 km<sup>2</sup>, a contributing  
138 drainage basin of 4080 km<sup>2</sup> and salinities ranging from 0 to 35‰ (Kjerfve et al., 1997).  
139 This bay is currently considered to be one of the most degraded estuarine systems off  
140 the Brazilian coast (Meniconi et al., 2012; Valentin et al., 1999). Itapanhaú River  
141 estuary, east of São Paulo state (Brazil) (23°49'47.1"S, 46°09'12.8"W), contributes to the  
142 Bertioga Channel, adjacent to Santos Bay, the largest port terminal of Latin America  
143 (Ambrozevicius and Abessa, 2008). It has a drainage basin of 260 km<sup>2</sup> (Bernardes and  
144 Miranda, 2001) and salinities ranging from 0 to 35‰ (Maciel, unpublished data).  
145 Paranaguá Estuarine Complex, located in coastal Paraná state (Brazil) (25°29'26.7"S,  
146 48°29'55.6"W), is divided into into north-south (Laranjeira and Pinheiro) and east-west  
147 (Paranaguá Bay) regions, with an area of 612 km<sup>2</sup> (Lana et al., 2001) and salinities  
148 ranging from 0 to 31‰ (Dias et al., 2016). La Plata Estuary is formed by the  
149 convergence of the Paraná and Uruguay rivers (Guerrero et al. 1997), between  
150 Argentina and Uruguay (34°30'S e 58°10'W). With an area of 35,000 km<sup>2</sup>, the estuary is  
151 the second largest fluvio-marine system in the Americas, with a contributing drainage  
152 basin area of 3,170,000 km<sup>2</sup>. Salinities range from 0 to 32‰ (Acha et al., 2008;  
153 Avigliano et al., 2017c).

## 155 2.2. Sampling

156 All sample specimens were obtained from small scale artisanal landings, except those  
157 from La Plata Estuary, Argentina (Paraná Guazú and Sauce rivers), which were  
158 collected by scientific collections using hook. Fishes were identified based on  
159 Marceniuk (2005) and Marceniuk and Menezes (2007) keys, measured (total length -  
160 TL,  $\pm 0.1$  cm) and the *lapillus* otoliths were removed, washed with ultrapure water, air  
161 dried and weighed ( $\pm 0.001$ g). Table 1 shows the biometrics information.

162

## 163 2.3. Otolith chemistry

164 *Genidens barbatus* left otoliths (Table 1) were decontaminated with 3% H<sub>2</sub>O<sub>2</sub>, 2% HNO<sub>3</sub>  
165 (Merck KGaA, Garmstadt, Germany) and washed with Milli-Q water (resistivity 18.2  
166 mOhm/cm), and dried (Avigliano et al., 2017d). Otoliths were inserted into epoxy resin,  
167 and 700  $\mu$ m thick central sections were obtained from cured mounts using a Buehler  
168 Isomet low speed saw (Hong Kong, China). The sections were fixed onto glass slides  
169 using epoxy resin, and the upper otolith surface polished with 10  $\mu$ m grit sandpaper and  
170 then thoroughly rinsed with Milli-Q water. As age may influence the chemical  
171 composition of calcified structures, annual otolith growth rings (Reis 1985b) were  
172 counted under magnification (40x) using a Leica EZ4-HD stereomicroscope. Laser  
173 Ablation Inductively Coupled Plasma Mass Spectrometry (LA-ICP-MS) was used to  
174 measure <sup>43</sup>Ca, <sup>24</sup>Mg, <sup>51</sup>V, <sup>55</sup>Mn, <sup>60</sup>Ni, <sup>63</sup>Cu, <sup>66</sup>Zn, <sup>85</sup>Rb, <sup>88</sup>Sr, <sup>107</sup>Ag, <sup>111</sup>Cd, <sup>138</sup>Ba, <sup>202</sup>Hg  
175 and <sup>208</sup>Pb in otolith cores and edges at the University of Texas at Austin Department of  
176 Geosciences (USA). The LA-ICP-MS system consisted in an ESI NWR193-UC  
177 excimer laser ablation system (193 nm, 4ns pulse width) coupled to an Agilent 7500ce  
178 ICP-MS. A rectangular aperture of 25x100  $\mu$ m was used at 8  $\mu$ m s<sup>-1</sup> (repetition rate/ of



179 10 Hz, energy densities/  $3.8 \text{ Jcm}^{-2}$ ). To minimize the temporal sampling alias, the long  
180 axis of the aperture was maintained parallel to growth banding in all the transects.  
181 Based on the growth ring chronologies, the sampled core and edge regions correspond  
182 to within the first year (inner 1,000-1,500  $\mu\text{m}$ ) and last two years (outer 300  $\mu\text{m}$ ) of life,  
183 respectively. Prior to measurements, the surface contaminants were removed by pre-  
184 ablation, using a spot size of  $25 \times 125 \mu\text{m}$  at  $50 \text{ m s}^{-1}$ . The ICP-MS was operated at  
185 power of 1600 W with using argon as carrier gas ( $800 \text{ mL min}^{-1}$ ). Ratios  
186  $^{232}\text{Th}^{16}\text{O}/^{232}\text{Th}$  ( $<0.35\%$ ) and  $^{238}\text{U}/^{232}\text{Th}$  ( $\sim 1$ ) were used during tuning to monitor the  
187 oxide production and mass fractionation plasma robustness. NIST 612 and USGS  
188 MACS-3 reference materials, analyzed in replicate each hour, were used as external and  
189 primary standards, respectively (Jochum et al., 2011).  
190 Analyte intensities were converted to elemental concentrations ( $\text{mg kg}^{-1}$ ) using Iolite  
191 software (Paton et al., 2011), with  $^{43}\text{Ca}$  (38.3 weight %) as the internal standard  
192 (Yoshinaga et al. 2000).  
193 Reference materials recoveries averaged and were within 7% of to GeoREM preferred  
194 values (Jochum et al. 2011): 98% for  $^{138}\text{Ba}$ , 106% for  $^{63}\text{Cu}$ , 96% for  $^{24}\text{Mg}$ , 103% for  
195  $^{55}\text{Mn}$ , 102% for  $^{60}\text{Ni}$ , 100% for  $^{88}\text{Sr}$  and 93% for  $^{66}\text{Zn}$ . Detection limits (LOD,  $\text{mg kg}^{-1}$ )  
196 based on three times the standard deviation of the estimated baseline intensity during  
197 bracketing gas blank intervals were 0.01 for  $^{138}\text{Ba}$ , 0.21 for  $^{63}\text{Cu}$ , 0.12 for  $^{24}\text{Mg}$ , 0.16 for  
198  $^{55}\text{Mn}$ , 0.07 for  $^{60}\text{Ni}$ , 0.01 for  $^{88}\text{Sr}$  and 0.28 for  $^{66}\text{Zn}$ . Concentrations were expressed as  
199 molar ratios in relation to Ca (element/Ca,  $\text{mmol mol}^{-1}$ ). Otolith  $^{51}\text{V}$ ,  $^{60}\text{Ni}$ ,  $^{63}\text{Cu}$ ,  $^{85}\text{Rb}$ ,  
200  $^{107}\text{Ag}$ ,  $^{111}\text{Cd}$ ,  $^{202}\text{Hg}$  and  $^{208}\text{Pb}$  levels were below LOD, thus, further data analysis is  
201 based on concentrations of Mg, Mn, Zn, Sr and Ba.

202

## 203 2.4. Otolith morphometry

204 Digital images of the distal face of *G. barbuis* right *lapilli* otoliths (Table 1) were  
205 recorded (Nikon Coolpix L110) at the same magnification against a black background  
206 with a scale.

207 Differences in otolith contour between estuaries were calculated using Elliptic Fourier  
208 Analysis (EFA), where otolith curvature was modeled as a two-dimensional closed  
209 curve applying a combination of harmonically related sine and cosine functions  
210 (descriptors), with each function composed of four Fourier Coefficients (FCs). The first  
211 12 harmonics obtained 99.99% of the accumulated power, according to the Fourier  
212 Power Spectrum (Crampton, 1995) (Figure 2). The first three descriptors were used to  
213 normalize the FCs, being converted into constants, totaling 45 FCs instead of 48. The  
214 FCs were calculated using the Shape 1.3 software.

215

## 216 **2.5. Statistical analysis**

217 A covariance analysis (ANCOVA) was used to verify the effect of total length (TL) on  
218 FCs. One FC (b8) co-varied with TL ( $F=4.0$ ,  $p=0.045$ ) and were corrected by  
219 subtracting the common slope of the ANCOVAs. To avoid potential allometric effects,  
220 FCs were normalized to TL using the allometric ratio and standardized to a fish length  
221 of 58.5 cm (mean TL for all fish) (Leonart et al. 2000). A principal component analysis  
222 (PCA) was performed to reduce the dimension of the morphometric data matrix (Tuset  
223 et al., 2020) and convert the 45 FCs into 11 independent principal components (PCs),  
224 created through the orthogonal combination of the original variables, which  
225 accumulated 99.9% of the variability. This process also reduces multi-collinearity  
226 between the FCs.

227 Shapiro-Wilk and Levene tests were performed to test elemental ratios for normality  
228 and homogeneity of variance, respectively. Spearman and ANCOVA correlation were

229 used to test the effect of age, TL and otolith weight on the element:Ca ratios (Longmore  
230 et al. 2010; Kerr and Campana 2014). Only Mg:Ca, Mn:Ca, Zn:Ca and Sr:Ca in the core  
231 co-varied with age ( $7.0 < F < 37$   $0.0001 < p < 0.01$ ) and this trend was removed by  
232 subtracting the common slope of the ANCOVAs. Since core Mg:Ca, Zn:Ca and Sr:Ca  
233 ratios fulfilled the assumptions of normality and homogeneity (Shapiro-Wilk and  
234 Levene tests,  $p > 0.05$ ), ANOVA and Tukey tests were used to make univariate  
235 comparisons between sampling sites. Core Mn:Ca and Ba:Ca ratios and edge  
236 elemental:Ca ratios did not meet the assumptions simultaneously (Shapiro-Wilk and  
237 Levene tests,  $p < 0.05$ ), so Kruskal Wallis was used for the same purpose.

238 Permutational multivariate analysis of variance (PERMANOVA) based on the distances  
239 of Mahalanobis with 9999 permutations (Anderson 2006) was used to evaluate otolith  
240 morphometric (PCs) and multi-elemental (core and edge separately) differences for each  
241 sampling site.

242 Discriminant analyses were performed to assess the ability of the data to be classified  
243 in their respective capture areas. Because the variance–covariance matrices were not  
244 homogeneous (Box test,  $p < 0.05$ ), quadratic models (QDA) instead of linear were  
245 applied to assess classification by otolith shape (PCs), otolith core and edge chemistry.  
246 An additional discriminant analysis (lineal model, LDA) was conducted using the  
247 otolith shape variables (PCs) and the edge elemental ratios together to determine if the  
248 integrated use of these two methods of stock assessment can improve discriminatory  
249 ability in relation to their independent use. LDA was used because co-variance matrices  
250 were homogeneous (Box test,  $p > 0.05$ ).

251 Prior to discriminant analyses, multi-collinearity was verified by using the tolerance and  
252 F-to-remove values (Hair et al., 2013). The classification accuracy of the QDA and  
253 LDA were tested by leave-one-out cross-validation (stepwise jackknifed procedure).

254 Finally, the expected prior probability classification (random rate) was estimated on  
255 sample sizes and group numbers, and then, proportion tests were performed to assess  
256 the difference between random and the percentage of correctly classified individuals.

257 Statistical analyses were performed using Mynstat 13 and SPSS 17.0 software.

### 258 3. Results

259

#### 260 3.1. Otolith chemistry

261 Three element:Ca ratios (Mg:Ca, Sr:Ca, Ba:Ca) were significantly different  
262 ( $p < 0.05$ ) between several sampling sites for otolith edge measurements (Figure 3),  
263 whereas no differences were observed for Mn:Ca ( $H = 2.98$ ;  $p = 0.5613$ ) and Zn:Ca ( $H =$   
264  $2.78$ ;  $p = 0.5950$ ). Otolith edge Mg:Ca was higher in Paranaguá Bay and lower in  
265 Paraíba do Sul River ( $H = 13.40$ ;  $p = 0.0095$ ). Edge Sr:Ca was higher in Paraíba do Sul  
266 River, Itapanhaú River and Paranaguá Bay, and lower in Guanabara Bay. Edge Ba:Ca  
267 ratio was high in La Plata Estuary and low in Guanabara Bay.

268 Multivariate analysis (PERMANOVA) based on otolith edge chemistry reveals  
269 significant differences between all sites ( $2.4 < F < 6.1$ ;  $0.003 < p < 0.22$ ), except for  
270 Itapanhaú River-Paranaguá Bay ( $F = 1.4$ ,  $p = 0.22$ ) and Paraíba do Sul River-Itapanhaú  
271 River ( $F = 1.8$ ,  $p = 0.09$ ). The first two axes of the QDA (Wilks's Lambda = 0.041,  $F = 22.7$ ,  
272  $p < 0.0001$ ) explained 97% of the variability, with the first axis being the most  
273 representative (93%). Based on means of standardized coefficients, the most relevant  
274 variables for classification were Ba/Ca (-1.1) and Sr/Ca (0.34) for the first function and  
275 Sr/Ca (0.93) and Zn/Ca (-0.29) for the second one.

276 Cross-classification matrix indicates that 61.3% of individuals were correctly  
277 classified. For the chemical analyses, expected prior probabilities of classification (in  
278 %) were 18, 24, 31, 8 and 7 for Paraíba do Sul River, Guanabara Bay, Itapanhaú River,

279 Paranaguá Bay and La Plata Estuary, respectively (Table 2). The percentage of  
280 classification was perfect (100%) for the La Plata Estuary and relatively high for  
281 Guanabara Bay (86.4%), indicating they are non-random outcomes (Table 2). For the  
282 other sites, low/moderate (33.3-55.5%) and no significant differences in  
283 classification rate were observed with respect to random (Table 2). However,  
284 misclassified individuals were assigned to geographically proximal sampling sites,  
285 except for La Plata Estuary.

286 Otolith core Mg:Ca was higher in Paraíba do Sul River and Itapanhaú River,  
287 intermediate in Guanabara and Paranaguá Bays and lower in La Plata Estuary ( $F= 13.0$ ;  
288  $p= 0.01$ ). Core Mn:Ca ratio was higher in La Plata Estuary and lower in the other  
289 sampling sites ( $H= 18.1$ ;  $p= 0.001$ ). Core Zn:Ca was higher in Paranaguá Bay and  
290 Paraíba do Sul River, intermediate in Guanabara Bay and Itapanhaú River and lower in  
291 La Plata Estuary ( $H= 11.2$ ;  $p= 0.02$ ). Sr:Ca was higher in Itapanhaú River and  
292 Paranaguá Bay, intermediate in Paraíba do Sul River and Guanabara Bay, and lower in  
293 La Plata Estuary ( $H= 27.0$ ;  $p<0.0001$ ). The highest core Ba:Ca values were found in  
294 specimens collected from Paraíba do Sul River and La Plata Estuary ( $H= 46.9$ ;  
295  $p<0.0001$ ).

296 PERMANOVA based on otolith core chemistry demonstrates significant differences  
297 between all sites ( $2.6<F<6.2$ ;  $0.0001<p<0.01$ ). The first two function of the QDA  
298 (Wilks's Lambda=0.088,  $F=14.9$ ,  $p<0.0001$ ) explained 83 and 7% of the variability,  
299 respectively (accumulate=90%). Ba/Ca (first function=0.69, second function=0.86) and  
300 Mn/Ca (first function=0.51, second function=-0.77) were the most important variables  
301 for the classification. The mean jackknifed classification percentage was 78.9% and like  
302 otolith edge, the classification percentage was 100% for the La Plata Estuary. The  
303 jackknifed percentages for the other sites ranged from 66.7 to 82.4%. All

304 jackknifed classification percentages were significantly higher than random (Table 2).  
305 Except for Paranaguá and Paraíba do Sul capture sites, misclassified individuals from  
306 other sites were classified into geographically close sampling sites.

307

### 308 **3.2. Otolith morphometry**

309 PERMANOVA showed significant difference in the otolith shape between all sampling  
310 sites ( $F=3.0$ ;  $0.0001 < p < 0.02$ ), except between Guanabara and Paranaguá bays, and  
311 between Itapanhaú River and Paranaguá Bay ( $0.051 < p < 0.12$ ).

312 According to the LDA (Lambda de Wilks=0.39,  $p < 0.0001$ ) the first two discriminant  
313 functions explained 51.3% and 21.9% (accumulate: 73.2%) of the variability,  
314 respectively.

315 The percentage of well-classified individuals (mean=45.9%) was relatively low for all  
316 sites (32.1-67.6%), except La Plata Estuary (67.6%). The prior probabilities of  
317 classification (random, in %) were 18 for Paraíba do Sul River, 26 for Guanabara Bay;  
318 19 for Itapanhaú River, 18 for Paranaguá Bay and 21 for La Plata Estuary. Re-  
319 classification rates were significantly higher than random for Paraíba do Sul River and  
320 La Plata estuary (Table 2).

321

### 322 **3.3. Simultaneous use of chemistry and morphometry**

323 According to LDA (Wilks's Lambda=0.05,  $F=11.7$ ,  $p < 0.0001$ ) based on the concomitant  
324 use of the two techniques, the mean classification percentage (58.2%) was intermediate  
325 in relation to that obtained when both methods were applied separately (Table 2). The  
326 LDA analysis had high jackknifed classification success for La Plata Estuary (100%),  
327 moderate success for Guanabara Bay (66.7%) and relatively low success for the other

328 sites (16.7-54.5%). Only Guanabara Bay and La Plata Estuary showed higher  
329 classification rates than chance (Table 2).

330

#### 331 **4. Discussion**

332 This study evaluated otolith microchemistry and shape for the first time as a potential  
333 integrated tool for discrimination of catfish stocks in Southwestern Atlantic estuarine  
334 settings, including two (Paraíba do Sul River and Itapanhaú River) estuaries that have  
335 not been considered in previous population structure evaluations. Multivariate analysis  
336 based on otolith chemistry proved effective for delimiting several capture sites. QDA  
337 based on edge chemistry was particularly effective for delimiting samples from La Plata  
338 Estuary and Guanabara Bay, while the other sites had low classification rates. The high  
339 classification rates obtained for La Plata Estuary (100%) and Guanabara Bay (86.4%)  
340 are consistent with previous studies, which reported values of 100% for Guanabara Bay  
341 (Avigliano et al., 2017d) and between 81.3% (Avigliano et al., 2019) and 100%  
342 (Avigliano et al., 2017d, 2015c) for La Plata Estuary. Although classification rates are  
343 sensitive to the variables used and the number of groups, the available evidence  
344 supports that different stocks reside within these two coastal systems.

345 Based on morphological and chemical analyzes, Paraíba do Sul, the northernmost site  
346 studied to date, showed a high overlap with the sites located to the south (Guanabara  
347 Bay, 500 km) and Paranaguá Bay (1,000 km), while high segregation was observed in  
348 relation to the more southern and remote (2,400 km). Itapanhaú River, one of the sites  
349 studied for the first time, had a high overlap with sites located to the north (Paraíba do  
350 Sul and Guanabara Bay), but showed high segregation in relation to the southernmost  
351 localities (Paranaguá Bay and La Plata Estuary). *G. barbatus* specimens from Paranaguá  
352 Bay (N=6) were mostly classified (misclassification=66.7%) in Itapanhaú River, but we

353 acknowledge that this could be a statistical artifact due to the relatively small sample  
354 size compared to other capture sites. Previous studies have reported classification  
355 percentages of 82-100% using otoliths (Avigliano et al., 2017d, 2019a) and 100% using  
356 spines (Avigliano et al., 2019c, 2020) for Paranaguá Bay. However, consistent with  
357 previous otolith and spine studies we observe no overlap with La Plata Estuary  
358 (Avigliano et al., 2020, 2019, 2017d) and relatively low (18%) overlap with Guanabara  
359 Bay (Avigliano et al., 2017d), which supports that the chemical signature of Paranaguá  
360 Bay can be distinguished from Guanabara Bay and La Plata Estuary.

361 The performance of both techniques applied simultaneously was lower than that of the  
362 chemistry used alone. This is probably due to the relatively low efficiency of  
363 morphometry to discriminate between some of the *G. barbuis* stocks (Table 2).  
364 However, when both techniques are moderately efficient to discriminate between  
365 stocks, the simultaneous use of these tends to increase the classification percentages  
366 (Biolé et al., 2019; Longmore, et al., 2010; Soeth et al., 2019), since the variables can  
367 respond to different drivers, for example environmental, physiological, genetic, or  
368 evolutionary (Avigliano, 2021; Tanner, et al., 2015).

369 The high overlap obtained here among the closest sites (e.g. Itapanhaú River and  
370 Paranaguá Bay, and Paraíba do Sul, Guanabara Bay and Paranaguá Bay) could be due  
371 to a high connectivity between these sampling sites, however, similar environmental or  
372 endogenous pressures (e.g. physiological factors) on these sites could contribute to  
373 similar chemical signatures in the region (Avigliano, 2021). A recent *G. genidens*  
374 otolith edge microchemical study found high misclassification rates (up to 52.6%)  
375 between Itapanhaú River and Paranaguá Bay (Maciel et al., 2020). These authors  
376 suggested that *G. genidens* presents low connectivity between the studied estuaries, so  
377 similar chemical fingerprints in the present study may indicate similar environmental



378 pressures rather than high connectivity.

379 Maciel et al. (2020) also found that otolith core-based classification rates (78.9%) for *G.*  
380 *barbus* were somewhat higher than edge-based classification rates (61.3%), suggesting  
381 some segregation between study sites. However, classification of adult fish based on the  
382 otolith cores should be taken with caution because the environment used by juveniles  
383 does not necessarily correspond to that in capture sites. Assuming that there is high  
384 segregation throughout ontogeny, differences in classification success between core and  
385 edge could be due to spatio-temporal environmental variations. For example, Avigliano  
386 et al. (2017a) demonstrated that temporal variation in the chemical signature of the adult  
387 catfish otolith core can affect the percentages of spatial classification.

388 Ba/Ca, Sr/Ca, Mn/Ca and Zn/Ca were the most important variables for delimiting  
389 groups. In several diadromous species, Ba/Ca and Sr/Ca can negatively and positively  
390 proxy salinity, rather than to other exogenous or endogenous factors (Brown and  
391 Severin, 2009), and thus have been widely used to track migratory routes in saline  
392 gradients (Araya et al., 2014; Hermann et al., 2016). Particularly in *G. barbus*, these  
393 element:Ca ratios in calcified structures were associated with salinity and surrounding  
394 water concentration (Avigliano et al., 2019), and have been useful in describing the life  
395 history patterns (Avigliano et al., 2017c, 2015b). The incorporation of Mn into the  
396 otolith can be regulated by both endogenous and exogenous factors, and is species-  
397 dependent (Hüssy et al., 2020; Sturrock et al., 2015). In some species such as  
398 *Micropogonias furnieri* (Avigliano, et al., 2021), *Micropogonias undulatus* (Altenritter  
399 et al., 2018; Dorval et al., 2007) and *Morone saxatilis* (Mohan et al., 2012), Mn/Ca has  
400 been linked with environmental concentration (Dorval et al., 2007; Mohan et al., 2012),  
401 while in *Gadus morhua*, *Platichthys flesus*, *Pseudopleuronectes americanus*, and *M.*  
402 *undulates*, it has been negatively associated to dissolved oxygen. Other factors such as

403 temperature, salinity, food composition and/or growth have also been identified as  
404 potential Mn drivers (Hüssy et al., 2020; Thomas and Swearer, 2019). For *G. barbuis*,  
405 Mn/Ca values are several times higher in the core than in the edge, as previously  
406 reported by (Avigliano et al., 2017d, 2017a), and similarly reported for other species  
407 (Limburg et al., 2015; Miller, 2009; Rogers et al., 2019), including *G. genidens* (Maciel  
408 et al., 2020) and other ariids like *Cathorops spixii* (Maichak de Carvalho et al., 2020).  
409 Mn enrichment in otolith cores has been linked to maternal transfer, transition to free-  
410 embryo or juvenile or growth (Hüssy et al., 2020). Literature on otolith Zn  
411 incorporation is scarce. Otolith Zn levels seem to be independent of environmental  
412 concentrations (Ranaldi and Gagnon, 2008), but may be influenced by diet (Ranaldi and  
413 Gagnon, 2008), growth (Hüssy et al., 2020; Sturrock et al., 2015), ontogeny (Avigliano  
414 et al., 2015a; Ranaldi and Gagnon, 2008) and gonadosomatic activity (Sturrock et al.,  
415 2015). In the present study, Zn/Ca values were comparable between core and  
416 spatially within the edge, and controlling factor are unclear.

417 Otolith shape is also affected for endogenous and exogenous factors (Reichenbacher et  
418 al., 2009; Vignon and Morat, 2010b), which may be expressed as inter and intra-specific  
419 morphometric differences. Quantitative characterization of these differences have been  
420 exploited in recent decades to study stock compositions (Biolé et al., 2019; Longmore,  
421 et al., 2010) and species delimitation (Avigliano et al., 2018; Tuset et al., 2013). Among  
422 the main environmental morphologic drivers are temperature, salinity, depth and diet  
423 (Lombarte and Leonart, 1993; Sea et al., 2008; Tuset et al., 2003; Vignon, 2018),  
424 however, genetics (Annabi et al., 2013; Reichenbacher and Reichard, 2014; Vignon and  
425 Morat, 2010b), growth rate and ontogeny (Vignon, 2012) can also affect morphology.  
426 In this study, multivariate analyses of otolith contours allowed partial site  
427 discrimination, particularly La Plata Estuary and marginally for Paraíba do Sul.

428 However, the otolith shape showed low discriminatory power and high overlap in both  
429 PERMANOVA and discriminant analysis, therefore, this methodology is not  
430 recommended for delimiting *G. barbuis* stocks, at least among the sampling sites from  
431 Brazil. Interestingly, EFA provide efficient for delimiting *G. genidens* catfish  
432 population between Paraíba do Sul River, Guanabara Bay and Paranaguá Bay (Maciel et  
433 al., 2020), suggesting that factors that regulate otolith shape are species-dependent  
434 within the genus. On the other hand, *G. genidens* is considered to be a less migratory  
435 species than *G. barbuis* (Maciel et al., 2020), remaining within estuaries throughout  
436 most of its life. This would not only reduce the chance of connectivity, but could reduce  
437 the variability of environments to which they are exposed, impacting on the otolith  
438 morphometry.

439 In summary, this work complements the evaluation of catfish population structure in the  
440 Southeastern Atlantic margin between latitude 21° and 34° S, by integrating otolith  
441 shape and microchemistry in previously studied and two new study sites. Otolith shape  
442 was not particularly useful for classification, whereas otolith microchemistry supported  
443 the site specific differences reported by previous studies, and shed light on the regional  
444 population structure as a whole. The results revealed on a smaller geographical scale  
445 (~300 km), microchemistry may confuse between some sampling sites, which could be  
446 revealing the limits of the method's discriminatory capacity or events of high  
447 connectivity. Synthesis of all findings supports the presence of different management  
448 units, corresponding to the La Plata Estuary, Lagoa dos Patos, Paranaguá-Itapanhaú  
449 River, and Paraíba do Sul-Guanabará. Future studies may improve population  
450 assessments of connectivity and distribution limits by including other methodologies,  
451 such as genetics, capture and recapture assessments.

452

## 453 5. Acknowledgements

454 We thank the CNPq, FAPERJ (MV) and CAPES (TM and BMC) for the research grants  
 455 and studentships. Funding was provided by National Council for Scientific and  
 456 Technological Development (CNPq), Ministry of Science, Technology, Innovations and  
 457 Communications (MCTIC) and Secretary of Aquaculture and Fisheries, Ministry of  
 458 Agriculture, Livestock and Food Supply (SAP-MAPA) (Call MCTI/MPA/CNPq N°  
 459 22/2015 - Process: 445782/2015-3), Agencia Nacional de Promoción Científica y  
 460 Tecnológica (Grant PICT 2015-1823), and Universidad de Buenos Aires (Grant  
 461 UBACyT 160 20020150100052BA).

462

## 463 6. References

- 464 Acha, E.M., Mianzan, H., Guerrero, R., Carreto, J., Giberto, D., Montoya, N., Carignan,  
 465 M., Marcelo Acha, E., Mianzan, H., Guerrero, R., Carreto, J., Giberto, D.,  
 466 Montoya, N., Carignan, M., 2008. An overview of physical and ecological  
 467 processes in the Rio de la Plata Estuary. *Cont. Shelf Res.* 28, 1579–1588.  
 468 <https://doi.org/10.1016/j.csr.2007.01.031>
- 469 Altenritter, M.E., Cohuo, A., Walther, B.D., 2018. Proportions of demersal fish exposed  
 470 to sublethal hypoxia revealed by otolith chemistry. *Mar. Ecol. Prog. Ser.* 589, 193–  
 471 208. <https://doi.org/10.3354/meps12469>
- 472 Ambrozevicius, A.P., Abessa, D.M.S., 2008. Acute toxicity of waters from the urban  
 473 drainage channels of Santos (São Paulo, Brazil). *Panam. J. Aquat. Sci.* 3, 108–115.
- 474 Annabi, A., Said, K., Reichenbacher, B., 2013. Inter-population differences in otolith  
 475 morphology are genetically encoded in the killifish *Aphanius fasciatus*  
 476 (Cyprinodontiformes). *Sci. Mar.* 77, 269–279.  
 477 <https://doi.org/10.3989/scimar.03763.02A>
- 478 Araya, M., Niklitschek, E.J., Secor, D.H., Piccoli, P.M., 2014. Partial migration in  
 479 introduced wild chinook salmon (*Oncorhynchus tshawytscha*) of southern Chile.  
 480 *Estuar. Coast. Shelf Sci.* 149, 1–9. <https://doi.org/10.1016/j.ecss.2014.07.011>
- 481 Avigliano, E., Alves, N., Rico, R., Ruarte, C., D'Atri, L., Méndez, A., Pisonero, J.,  
 482 Volpedo, A., Borstelmann, C., 2021. Population structure and ontogenetic habitat  
 483 use of *Micropogonias furnieri* in the southwestern Atlantic Ocean inferred by  
 484 otolith chemistry. *Fish. Res.* 204, 105953.
- 485 Avigliano, E., Carvalho, B.M., Leisen, M., Romero, R., Velasco, G., Vianna, M., Barra,  
 486 F., Volpedo, A.V., 2017. Otolith edge fingerprints as approach for stock  
 487 identification of *Genidens barbuis*. *Estuar. Coast. Shelf Sci.* 194, 92–96.  
 488 <https://doi.org/10.1016/j.ecss.2017.06.008>
- 489 Avigliano, E., 2021. Optimizing the methodological design in fish stock delineation  
 490 from otolith chemistry: review of spatio-temporal analysis scales. *Rev. Fish. Sci.*  
 491 *Aquac.* in press.
- 492 Avigliano, E., Carvalho, B., Velasco, G., Tripodi, P., Vianna, M., Volpedo, A.V., 2016.  
 493 Nursery areas and connectivity of the adults anadromous catfish (*Genidens barbuis*)  
 494 revealed by otolith-core microchemistry in the south-western Atlantic Ocean. *Mar.*

- 495 Freshw. Res. 68, 931–940. <https://doi.org/10.1071/MF16058>
- 496 Avigliano, E., Carvalho, B., Velasco, G., Tripodi, P., Volpedo, A.V., 2017a. Inter-  
497 annual variability in otolith chemistry of catfish *Genidens barbatus* from South-  
498 western Atlantic estuaries. J. Mar. Biol. Assoc. United Kingdom.  
499 <https://doi.org/10.1017/S0025315417000212>
- 500 Avigliano, E., Carvalho, B.M., Miller, N., Gironde, S.C., Tombari, A., Limburg, K.E.,  
501 Volpedo, A.V., 2019. Fin spine chemistry as a non-lethal alternative to otoliths for  
502 stock discrimination in an endangered catfish. Mar. Ecol. Prog. Ser. 614, 147–157.  
503 <https://doi.org/10.3354/meps12895>
- 504 Avigliano, E., Domanico, A., Sánchez, S., Volpedo, A. V., 2017b. Otolith elemental  
505 fingerprint and scale and otolith morphometry in *Prochilodus lineatus* provide  
506 identification of natal nurseries. Fish. Res. 186, 1–10.  
507 <https://doi.org/10.1016/j.fishres.2016.07.026>
- 508 Avigliano, E., Leisen, M., Romero, R., Carvalho, B., Velasco, G., Vianna, M., Barra, F.,  
509 Volpedo, A.V., 2017c. Fluvio-marine travelers from South America: Cyclic  
510 amphidromy and freshwater residency, typical behaviors in *Genidens barbatus*  
511 inferred by otolith chemistry. Fish. Res. 193, 184–194.  
512 <https://doi.org/10.1016/j.fishres.2017.04.011>
- 513 Avigliano, E., Maichak de Carvalho, B., Leisen, M., Romero, R., Velasco, G., Vianna,  
514 M., Barra, F., Volpedo, A.V., 2017d. Otolith edge fingerprints as approach for  
515 stock identification of *Genidens barbatus*. Estuar. Coast. Shelf Sci. 194, 92–96.  
516 <https://doi.org/10.1016/j.ecss.2017.06.008>
- 517 Avigliano, E., Martinez, C.F.R., Volpedo, A.V., 2014. Combined use of otolith  
518 microchemistry and morphometry as indicators of the habitat of the silverside  
519 (*Odontesthes bonariensis*) in a freshwater-estuarine environment. Fish. Res. 149,  
520 55–60. <https://doi.org/10.1016/j.fishres.2013.09.013>
- 521 Avigliano, E., Miller, N., Maichak fr Carvalho, B., Córdoba, S., Tombari, A., Volpedo,  
522 V.A., 2020. Fin spine metals by LA-ICP-MS as a method for fish stock  
523 discrimination of *Genidens barbatus* in anthropized estuaries. Fish. Res. 230,  
524 105625. <https://doi.org/10.1016/j.fishres.2020.105625>
- 525 Avigliano, E., Pisonero, J., Méndez, A., Tombari, A., Volpedo, A. V., 2021. Habitat use  
526 of the amphidromous catfish *Genidens barbatus*: first insights at its southern  
527 distribution limit. New Zeal. J. Mar. Freshw. Res. 0, 1–7.  
528 <https://doi.org/10.1080/00288330.2021.1879178>
- 529 Avigliano, E., Rolón, M.E., Rosso, J.J., Mabrugaña, E., Volpedo, A.V., 2018. Using  
530 otolith morphometry for the identification of three sympatric and morphologically  
531 similar species of *Astyanax* from the Atlantic Rain Forest (Argentina). Environ.  
532 Biol. Fishes. <https://doi.org/10.1007/s10641-018-0779-2>
- 533 Avigliano, E., Saez, M.B., Rico, R., Volpedo, A. V., 2015a. Use of otolith  
534 strontium:calcium and zinc:calcium ratios as an indicator of the habitat of  
535 *Percophis brasiliensis* Quoy and Gaimard, 1825 in the southwestern Atlantic  
536 Ocean. Neotrop. Ichthyol. 13, 187–194. [https://doi.org/10.1590/1982-0224-](https://doi.org/10.1590/1982-0224-20130235)  
537 [20130235](https://doi.org/10.1590/1982-0224-20130235)
- 538 Avigliano, E., Velasco, G., Volpedo, A.V., 2015b. Assessing the use of two  
539 southwestern Atlantic estuaries by different life cycle stages of the anadromous  
540 catfish *Genidens barbatus* (Lacépède, 1803) as revealed by Sr:Ca and Ba:Ca ratios in  
541 otoliths. J. Appl. Ichthyol. 31, 740–743. <https://doi.org/10.1111/jai.12766>
- 542 Avigliano, E., Velasco, G., Volpedo, A.V., 2015c. Use of lapillus otolith  
543 microchemistry as an indicator of the habitat of *Genidens barbatus* from different  
544 estuarine environments in the southwestern Atlantic Ocean. Environ. Biol. Fishes

- 545 98, 1623–1632. <https://doi.org/10.1007/s10641-015-0387-3>
- 546 Avigliano, E., Villatarco, P., Volpedo, A.V., 2015d. Otolith Sr:Ca ratio and  
547 morphometry as indicators of habitat of a euryhaline species: The case of the  
548 silverside *Odontesthes bonariensis*. *Ciencias Mar.* 41, 189–202.  
549 <https://doi.org/10.7773/cm.v41i3.2464>
- 550 Bailey, D.S., Fairchild, E., Kalnejais, L.H., 2015. Microchemical signatures in juvenile  
551 winter flounder otoliths provide identification of natal nurseries. *Trans. Am. Fish.*  
552 *Soc.* 144, 173–183. <https://doi.org/10.1080/00028487.2014.982259>
- 553 Barletta, M., Lima, A.R.A., 2019. Systematic review of fish ecology and anthropogenic  
554 impacts in South American estuaries: Setting priorities for ecosystem conservation.  
555 *Front. Mar. Sci.* 6, 1–29. <https://doi.org/10.3389/fmars.2019.00237>
- 556 Begg, G.A., Waldman, J.R., 1999. An holistic approach to fish stock identification.  
557 *Fish. Res.* 43, 35–44. [https://doi.org/10.1016/S0165-7836\(99\)00065-X](https://doi.org/10.1016/S0165-7836(99)00065-X)
- 558 Bernardes, M.E.C., Miranda, L.B., 2001. Circulação estacionária e estratificação de sal  
559 em canais estuarinos: simulação com modelos analíticos. *Rev. Bras. Oceanogr.* 49,  
560 115–132. <https://doi.org/10.1590/S1413-77392001000100010>
- 561 Bernini, E., Rezende, C.E., 2004. Estrutura da vegetação em florestas de mangue do  
562 estuário do rio Paraíba do Sul, Estado do Rio de Janeiro, Brasil. *Acta Bot. Brasilica*  
563 18, 491–502. <https://doi.org/10.1590/S0102-33062004000300009>
- 564 Biolé, F.G., Thompson, G.A., Vargas, C. V., Leisen, M., Barra, F., Volpedo, A.V.,  
565 Avigliano, E., 2019. Fish stocks of *Urophycis brasiliensis* revealed by otolith  
566 fingerprint and shape in the Southwestern Atlantic Ocean. *Estuar. Coast. Shelf Sci.*  
567 229, 106406. <https://doi.org/10.1016/j.ecss.2019.106406>
- 568 Brown, R.J., Severin, K.P., 2009. Otolith chemistry analyses indicate that water Sr:Ca is  
569 the primary factor influencing otolith Sr:Ca for freshwater and diadromous fish but  
570 not for marine fish. *Can. J. Fish. Aquat. Sci.* 66, 1790–1808.  
571 <https://doi.org/10.1139/F09-112>
- 572 Caille, G.M., Ferrari, S., Albrieu, C., 1995. Los peces de la Ría de Gallegos, Santa  
573 Cruz, Argentina. *Nat. Patagónica, Ciencias Biológicas* 3, 191–194.
- 574 Campana, S.E., 1999. Chemistry and composition of fish otoliths: Pathways,  
575 mechanisms and applications. *Mar. Ecol. Prog. Ser.* 188, 263–297.  
576 <https://doi.org/10.3354/meps188263>
- 577 Clarke, L.M., Conover, D.O., Thorrold, S.R., 2011. Population differences in otolith  
578 chemistry have a genetic basis in menidia menidia. *Can. J. Fish. Aquat. Sci.* 68,  
579 105–114. <https://doi.org/10.1139/F10-147>
- 580 Crampton, J.S., 1995. Elliptic Fourier shape analysis of fossil bivalves: some practical  
581 considerations. *Lethaia* 28, 179–186. <https://doi.org/10.1111/j.1502-3931.1995.tb01611.x>
- 582
- 583 Dias, T.H., Oliveira, J., Sanders, C.J., Carvalho, F., Sanders, L.M., Machado, E.C., Sá,  
584 F., 2016. Radium isotope ( $^{223}\text{Ra}$ ,  $^{224}\text{Ra}$ ,  $^{226}\text{Ra}$  and  $^{228}\text{Ra}$ ) distribution near Brazil's  
585 largest port, Paranaguá Bay, Brazil. *Mar. Pollut. Bull.* 111, 443–448.  
586 <https://doi.org/10.1016/j.marpolbul.2016.07.004>
- 587 Dorval, E., Jones, C.M., Hannigan, R., Montfrans, J. van, 2007. Relating otolith  
588 chemistry to surface water chemistry in a coastal plain estuary. *Can. J. Fish. Aquat.*  
589 *Sci.* 64, 411–424. <https://doi.org/10.1139/f07-015>
- 590 Elsdon, T.S., Gillanders, B.M., 2003. Relationship between water and otolith elemental  
591 concentrations in juvenile black bream *Acanthopagrus butcheri*. *Mar. Ecol. Prog.*  
592 *Ser.* 260, 263–272. <https://doi.org/10.3354/meps260263>
- 593 Gomes, I.D., Araújo, F.G., 2004. Reproductive biology of two marine catfishes  
594 (*Siluriformes*, *Ariidae*) in the Sepetiba Bay, Brazil. *Rev. Biol. Trop.* 52, 143–156.



- 595 <https://doi.org/10.15517/rbt.v52i1.14763>
- 596 Gut, C., Vukić, J., Šanda, R., Moritz, T., Reichenbacher, B., 2020. Identification of past  
597 and present gobies: distinguishing *Gobius* and *Pomatoschistus* (Teleostei:  
598 Gobioidae) species using characters of otoliths, meristics and body morphometry.  
599 *Contrib. to Zool.* 89, 282–323. <https://doi.org/10.1163/18759866-BJA10002>
- 600 Hair, J.F., Black, W.C., Babin, B.J., Anderson, R.E., 2013. *Multivariate Data Analysis:*  
601 *Pearson New International Edition.* Pearson new international edition, Harlow,  
602 United Kingdom. <https://doi.org/10.1016/j.ijpharm.2011.02.019>
- 603 Hermann, T.W., Stewart, D.J., Limburg, K.E., Castello, L., 2016. Unravelling the life  
604 history of Amazonian fishes through otolith microchemistry. *R. Soc. Open Sci.* 3,  
605 160206. <https://doi.org/10.1098/rsos.160206>
- 606 Hüsey, K., Limburg, K.E., Pontual, H. De, Thomas, O.R.B., Cook, K., Heimbrand, Y.,  
607 Blass, M., Sturrock, A.M., 2020. Element patterns in otoliths: the role of  
608 biomineralization. *Rev. Fish. Sci. Aquac.* 1–33.  
609 <https://doi.org/10.1080/23308249.2020.1760204>
- 610 Hüsey, K., Mosegaard, H., Albertsen, C.M., Nielsen, E.E., Hemmer-Hansen, J., Eero,  
611 M., 2016. Evaluation of otolith shape as a tool for stock discrimination in marine  
612 fishes using Baltic Sea cod as a case study. *Fish. Res.* 174, 210–218.  
613 <https://doi.org/10.1016/J.FISHRES.2015.10.010>
- 614 Ibáñez, A.L., Hernández-Fraga, K., Alvarez-Hernández, S., 2017. Discrimination  
615 analysis of phenotypic stocks comparing fish otolith and scale shapes. *Fish. Res.*  
616 185, 6–13. <https://doi.org/10.1016/j.fishres.2016.09.025>
- 617 Jochum, K.P., Weis, U., Stoll, B., Kuzmin, D., Yang, Q., Raczek, I., Jacob, D.E.,  
618 Stracke, A., Birbaum, K., Frick, D.A., Günther, D., Enzweiler, J., 2011.  
619 Determination of reference values for NIST SRM 610-617 glasses following ISO  
620 guidelines. *Geostand. Geoanalytical Res.* 35, 397–429.  
621 <https://doi.org/10.1111/j.1751-908X.2011.00120.x>
- 622 Kerr, L.A., Campana, S.E., 2014. Chemical composition of fish hard parts as a natural  
623 marker of fish stocks, in: *Stock Identification Methods: Applications in Fishery*  
624 *Science: Second Edition.* Academic Press., San Diego, USA, pp. 205–234.  
625 <https://doi.org/10.1016/B978-0-12-397003-9.00011-4>
- 626 Kime, D.E., 1995. The effects of pollution on reproduction in fish. *Rev. Fish Biol. Fish.*  
627 5, 52–95. <https://doi.org/10.1007/BF01103366>
- 628 Kjerfve, B., Ribeiro, C.H.A., Dias, G.T.M., Filippo, A.M., Quaresma, V.S., 1997.  
629 Oceanographic characteristics of an impacted coastal bay: Baía de Guanabara, Rio  
630 de Janeiro, Brazil. *Cont. Shelf Res.* 17, 1609–1643.
- 631 Krüger, G.C.T., Carvalho, C.E.V., Suzuki, M.S., 2006. Dissolved nutrient, chlorophyll-  
632 a and DOC dynamic under distinct riverine discharges and tidal cycles regimes at  
633 the Paraíba do Sul River estuary, RJ, Brazil. *J. Coast. Res.* II, 724–730.
- 634 Lana, P.C., Marone, E., Lopes, R.M., Machado, E.C., 2001. The subtropical estuarine  
635 complex of Paranaguá Bay, Brazil. *Ecol. Stud.* 144, 131–145.  
636 [https://doi.org/10.1007/978-3-662-04482-7\\_11](https://doi.org/10.1007/978-3-662-04482-7_11)
- 637 Limburg, K.E., Walther, B.D., Lu, Z., Jackman, G., Mohan, J., Walther, Y., Nissling,  
638 A., Weber, P.K., Schmitt, A.K., 2015. In search of the dead zone: Use of otoliths  
639 for tracking fish exposure to hypoxia. *J. Mar. Syst.* 141, 167–178.  
640 <https://doi.org/10.1016/j.jmarsys.2014.02.014>
- 641 Lombarte, A., Leonart, J., 1993. Otolith size changes related with body growth, habitat  
642 depth and temperature. *Environ. Biol. Fishes* 37, 297–306.  
643 <https://doi.org/10.1007/BF00004637>
- 644 Longmore, C., Fogarty, K., Neat, F., Brophy, D., Trueman, C., Milton, A., Mariani, S.,

- 645 2010. A comparison of otolith microchemistry and otolith shape analysis for the  
646 study of spatial variation in a deep-sea teleost, *Coryphaenoides rupestris*. Environ.  
647 Biol. Fishes 89, 591–605. <https://doi.org/10.1007/s10641-010-9674-1>
- 648 López, R.B., Bellisio, N.B., 1965. Contribución al conocimiento del *Tachysurus barbatus*  
649 (Lacépède), bagre del Mar argentino (Pisces, Ariidae), in: Anuario Del II Congreso  
650 Latinoamericano Zoología. São Paulo, pp. 145–153.
- 651 Maciel, T.R., Avigliano, E., Maichak de Carvalhoc, B., Miller, N., Viannaa, M., 2020.  
652 Population structure and habitat connectivity of *Genidens genidens* (Siluriformes)  
653 in tropical and subtropical coasts from Southwestern Atlantic. Estuar. Coast. Shelf  
654 Sci. 242, 106839.
- 655 Maciel, T.R., Vaz-dos-Santos, A.M., Barradas, J.R.S., Vianna, M., 2019. Sexual  
656 dimorphism in the catfish *Genidens genidens* (Siluriformes: Ariidae) based on  
657 otolith morphometry and relative growth. Neotrop. Ichthyol. 17, e180101[1]-  
658 e180101[8]. <https://doi.org/10.1590/1982-0224-20180101>
- 659 Maichak de Carvalho, B., Pisonero, J., Mendez, A., Volpedo, A. V., Avigliano, E.,  
660 2020. Spatial environmental variability of natural markers and habitat use of  
661 *Cathorops spixii* in a neotropical estuary from otolith chemistry. J. Mar. Biol.  
662 Assoc. UK 100, 783–793.
- 663 Marceniuk, A.P., 2005. Chave para identificação das espécies de bagres marinhos  
664 (Siluriformes, Ariidae) da costa brasileira. Bol. do Inst. Pesca 31, 89–101.
- 665 Marceniuk, A.P., Menezes, N.A., 2007. Systematics of the family Ariidae  
666 (Ostariophysi, Siluriformes), with a redefinition of the genera, Zootaxa.  
667 <https://doi.org/10.11646/zootaxa.1416.1.1>
- 668 Mendonça, J.T., Quito, L., Jankowsky, M., Balanin, S., Neto, D.G., 2017. Diagnóstico  
669 da pesca do bagre-branco (*Genidens barbatus* e *G. planifrons*) NO LITORAL  
670 Sudeste-sul do Brasil: subsídios para o ordenamento. Inst. Pesca, São Paulo. 77.
- 671 Meniconi, M.F.G., Silva, T.A., Fonseca, M.L., Lima, S.O.F., Lima, E.F.A., Lavrado,  
672 H.P., Figueiredo-Jr., A.G., 2012. Baía de Guanabara: Síntese do conhecimento  
673 ambiental. Biodiversidade. Petrobras, Rio de Janeiro.
- 674 Miller, J.A., 2009. The effects of temperature and water concentration on the otolith  
675 incorporation of barium and manganese in black rockfish *Sebastes melanops*. J.  
676 Fish Biol. 75, 39–60. <https://doi.org/10.1111/j.1095-8649.2009.02262.x>
- 677 MMA, 2014. Portaria MMA Número 445, DOU: Brasília. Brazil.
- 678 Mohan, J.A., Rulifson, R.A., Reide Corbett, D., Halden, N.M., 2012. Validation of  
679 oligohaline elemental otolith signatures of striped bass by use of *in situ* caging  
680 experiments and water chemistry. Mar. Coast. Fish. 4, 57–70.  
681 <https://doi.org/10.1080/19425120.2012.656533>
- 682 Morales-Nin, B., 2000. Review of the growth regulation processes of otolith daily  
683 increment formation. Fish. Res. 46, 53–67. [https://doi.org/10.1016/S0165-7836\(00\)00133-8](https://doi.org/10.1016/S0165-7836(00)00133-8)
- 684
- 685 Patterson, W.F., Cowan, J.H., Wilson, C.A., Chen, Z., 2008. Temporal and spatial  
686 variability in juvenile red snapper otolith elemental signatures in the Northern Gulf  
687 of Mexico. Trans. Am. Fish. Soc. 137, 521–532. <https://doi.org/10.1577/T06-264.1>
- 688 Perin, S., Vaz-dos-Santos, A.M., 2014. Morphometry and relative growth of the  
689 Brazilian sardine, *Sardinella brasiliensis* (Steindachner, 1879) in the southeastern  
690 Brazilian bight. Arq. Zool. 45, 63–72.
- 691 Ranaldi, M.M., Gagnon, M.M., 2008. Zinc incorporation in the otoliths of juvenile pink  
692 snapper (*Pagrus auratus* Forster): The influence of dietary versus waterborne  
693 sources. J. Exp. Mar. Bio. Ecol. 360, 56–62.  
694 <https://doi.org/10.1016/j.jembe.2008.03.013>



- 695 Reichenbacher, B., Feulner, G.R., Tanja, S.M., 2009. Geographic variation in otolith  
696 morphology among freshwater populations of *Aphanius dispar* (Teleostei,  
697 Cyprinodontiformes) from the Southeastern Arabian Peninsula. *J. Morphol.* 270,  
698 469–484. <https://doi.org/10.1002/jmor.10702>
- 699 Reichenbacher, B., Reichard, M., 2014. Otoliths of five extant species of the annual  
700 killifish *Nothobranchius* from the east African Savannah. *PLoS One* 9, e112459.  
701 <https://doi.org/10.1371/journal.pone.0112459>
- 702 Reis, E.G., 1986a. Reproduction and feeding habits of the marine catfish, *Netuma barba*  
703 (Siluriformes, Ariidae), in the estuary of the Patos Lagoon (Brazil). *Atlântica* 8,  
704 35–55.
- 705 Reis, E.G., 1986b. A pesca artesanal de bagres marinhos (Siluriformes: Ariidae) no  
706 estuário da Lagoa dos Patos, RS, Brasil. Rio Grande.
- 707 Rogers, T.A., Fowler, A.J., Steer, M.A., Gillanders, B.M., 2019. Discriminating natal  
708 source populations of a temperate marine fish using larval otolith chemistry. *Front.*  
709 *Mar. Sci.* 6, 1–17. <https://doi.org/10.3389/fmars.2019.00711>
- 710 Sea, I., Brophy, D., King, P.A., 2008. Otolith shape analysis: its application for  
711 discriminating between stocks of Irish Sea and Celtic Sea herring (*Clupea*  
712 *harengus*) in the Irish Sea. *ICES J. Mar. Sci.* 65, 1670–1675.
- 713 Soeth, M., Spach, H.L., Daros, F.A., Adelir-Alves, J., de Almeida, A.C.O., Correia,  
714 A.T., 2019. Stock structure of Atlantic spadefish *Chaetodipterus faber* from  
715 Southwest Atlantic Ocean inferred from otolith elemental and shape signatures.  
716 *Fish. Res.* 211, 81–90. <https://doi.org/10.1016/j.fishres.2018.11.003>
- 717 Sturrock, A.M., Hunter, E., Milton, J.A., Johnson, R.C., Waring, C.P., Trueman, C.N.,  
718 EIMF, 2015. Quantifying physiological influences on otolith microchemistry.  
719 *Methods Ecol. Evol.* 6, 806–816. <https://doi.org/10.1111/2041-210X.12381>
- 720 Tanner, S., Reis-Santos, P., Cabral, H.N., 2015. Otolith chemistry in stock delineation:  
721 A brief overview, current challenges and future prospects. *Fish. Res.* 173, 206–  
722 213. <https://doi.org/10.1016/j.fishres.2015.07.019>
- 723 Thomas, O.R.B., Swearer, S.E., 2019. Otolith Biochemistry—A Review. *Rev. Fish. Sci.*  
724 *Aquac.* 27, 458–489. <https://doi.org/10.1080/23308249.2019.1627285>
- 725 Tuset, V.M., Galimany, E., Farrés, A., Marco-Herrero, E., Otero-Ferrer, J.L., Lombarte,  
726 A., Ramón, M., 2020. Recognising mollusc shell contours with enlarged spines:  
727 Wavelet vs Elliptic Fourier analyses. *Zoology* 140, 125778.  
728 <https://doi.org/10.1016/j.zool.2020.125778>
- 729 Tuset, V.M., Lozano, I.J., González, J.A., Pertusa, J.F., García-Díaz, M.M., 2003. Shape  
730 indices to identify regional differences in otolith morphology of comber, *Serranus*  
731 *cabrilla* (L., 1758). *J. Appl. Ichthyol.* 19, 88–93. <https://doi.org/10.1046/j.1439-0426.2003.00344.x>
- 733 Tuset, V.M., Parisi-Baradad, V., Lombarte, A., 2013. Application of otolith mass and  
734 shape for discriminating scabbardfishes *Aphanopus* spp. in the north-eastern  
735 Atlantic Ocean. *J. Fish Biol.* 82, 1746–1752. <https://doi.org/10.1111/jfb.12101>
- 736 Valentin, J.L., Tenenbaum, D.R., Bonecker, A.C.T., Bonecker, S.L.C., Nogueira, C.R.,  
737 Villac, M.C., 1999. O sistema planctônico da Baía de Guanabara: Síntese do  
738 conhecimento, in: Silva, S.H.G., Lavrado, H.P. (Eds.), *Ecologia dos ambientes*  
739 *costeiros do estado do Rio de Janeiro. Oecologia Brasiliensis*, Rio de Janeiro, pp.  
740 35–59. <https://doi.org/10.4257/oeco.1999.0701.02>
- 741 Velasco, G., Reis, E.G., Vieira, J.P., 2007. Calculating growth parameters of *Genidens*  
742 *barbus* (Siluriformes, Ariidae) using length composition and age data. *J. Appl.*  
743 *Ichthyol.* 23, 64–69. <https://doi.org/10.1111/j.1439-0426.2006.00793.x>
- 744 Vignon, M., 2018. Short-term stress for long-lasting otolith morphology — brief

- 745 embryological stress disturbance can reorient otolith ontogenetic trajectory. *Can. J.*  
746 *Fish. Aquat. Sci.* 75, 10. <https://doi.org/10.1139/cjfas-2017-0110>
- 747 Vignon, M., 2012. Ontogenetic trajectories of otolith shape during shift in habitat use:  
748 Interaction between otolith growth and environment. *J. Exp. Mar. Bio. Ecol.* 420–  
749 421, 26–32. <https://doi.org/10.1016/j.jembe.2012.03.021>
- 750 Vignon, M., Morat, F., 2010a. Environmental and genetic determinant of otolith shape  
751 revealed by a non-indigenous tropical fish. *Mar. Ecol. Prog. Ser.* 411, 231–241.  
752 <https://doi.org/10.3354/meps08651>
- 753 Vignon, M., Morat, F., 2010b. Environmental and genetic determinant of otolith shape  
754 revealed by a non-indigenous tropical fish. *Mar. Ecol. Prog. Ser.* 411, 231–241.  
755 <https://doi.org/10.3354/meps08651>
- 756
- 757

758 **Figure 1:** Map of the study area in the Southwest Atlantic Ocean. Red arrows indicate  
759 the approximate sampling region of *Genidens barbatus*.

760

761 **Figure 2:** Relationship between the descriptors and the accumulated Fourier Power  
762 Spectrum for *Genidens barbatus* otoliths. The first 12 harmonics reached 99.99% of the  
763 accumulated power.

764

765 **Figure 3:** *Genidens barbatus* otolith edge and core elemental ratios mean  $\pm$  SD  
766 (mmol/mol) for sampling sites. Distinct letters show significant differences between  
767 sites ( $p < 0.05$ ). PSR- Paraíba do Sul River; GB- Guanabara Bay; IR- Itapanhaú River;  
768 PB- Paranaguá Bay; PE- La Plata Estuary.

769

770 **Table 1:** Descriptive statistics of *Genidens barbuis* study specimens (mean and SD)  
 771 used for chemical (N, sample size=72) and morphometric (N=159) analysis. The  
 772 specimens used for the chemical analyzes were subsampled at random from the total  
 773 sample pool (N=159). TL= total length (cm); W = weight (g); SD =standard deviation;  
 774 Age = age in years.

Site	N	TL ± SD	W ± SD	Age ± SD
Chemistry				
Paraíba do Sul River	17	61.1 ± 7.3	2265 ± 950	13.4 ± 2.2
Guanabara Bay	22	62.2 ± 8.7	2870 ± 1445	14.0 ± 2.0
Itapanhaú River	22	61.5 ± 5.4	2371 ± 699	14.2 ± 1.9
Paranaguá Bay	6	49.9 ± 9.1	2058 ± 1201	9.8 ± 1.0
La Plata Estuary	5	65.0 ± 4.5	2861 ± 714	11.8 ± 1.1
Elliptic Fourier Analysis				
Paraíba do Sul River	28	62.8 ± 11.9	2742 ± 1720	
Guanabara Bay	38	62.2 ± 11.4	2925 ± 1677	
Itapanhaú River	31	61.7 ± 7.0	2544 ± 805	
Paranaguá Bay	28	48.8 ± 7.8	2295 ± 1291	
La Plata Estuary	34	55.8 ± 6.1	1700 ± 722	

775

776

777 **Table 2** Cross-classification matrices of the discriminant analyzes based on for *Genidens barbuis* otolith morphometry and microchemistry. The  
 778 numbers represent the classification percentage. N: sample size; PSR: Paraíba do Sul; GB: Guanabara; IR: Itapanhaú; PG: Itapanhaú; RDP: Río  
 779 de la Plata.

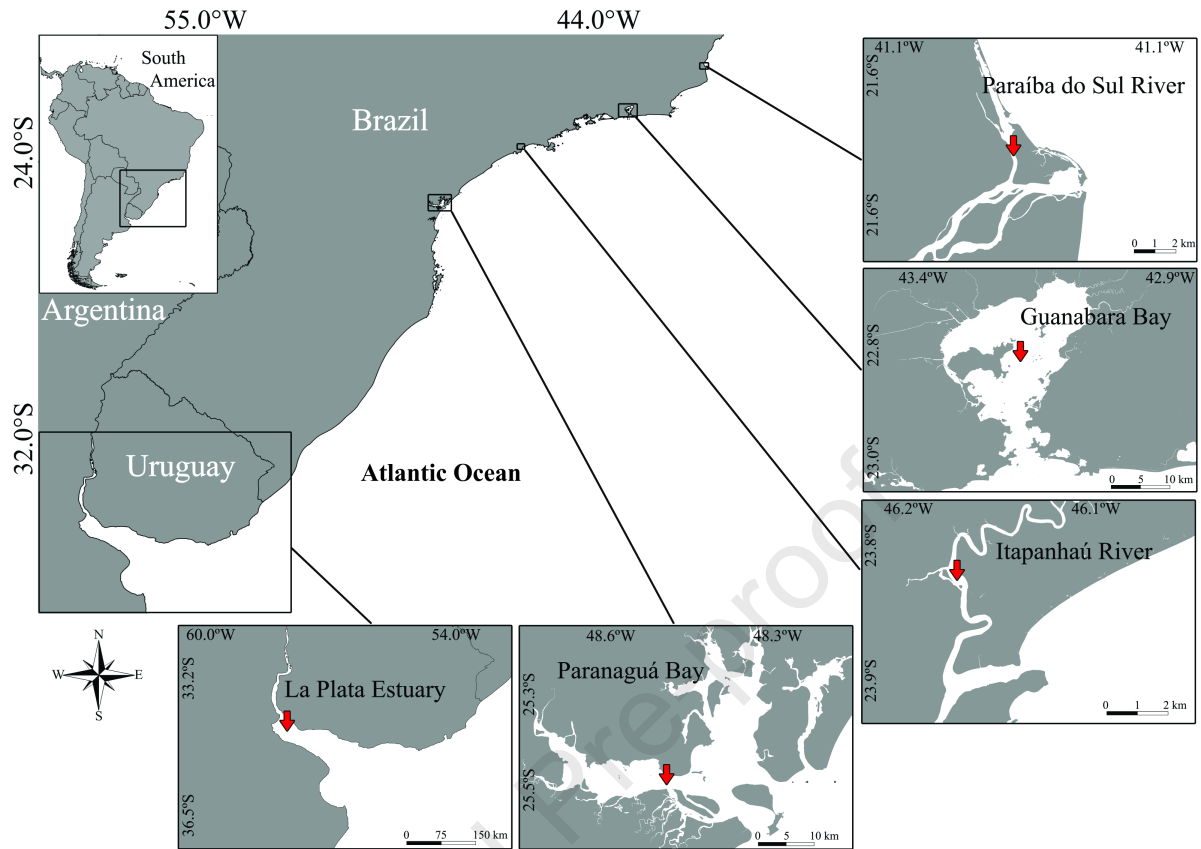
	Paraíba do Sul	Guanabara	Itapanhaú	Itapanhaú	Río de la Plata	N	Random (%)	p
<b>Shape (QDA)</b>								
<b>PSR</b>	<b>42.9</b>	17.9	17.9	7.1	14.3	28	18	0.04*
<b>GB</b>	18.4	<b>44.7</b>	5.3	15.8	15.8	38	24	0.09
<b>IR</b>	12.9	16.1	<b>38.7</b>	19.4	12.9	31	19	0.17
<b>PG</b>	7.1	21.4	21.4	<b>32.1</b>	17.9	28	18	0.23
<b>RDP</b>	5.9	8.8	5.9	11.8	<b>67.6</b>	34	21	<0.0001*
<i>Mean</i>					45.2			
<b>Edge (QDA)</b>								
<b>PSR</b>	<b>41.2</b>	23.5	29.4	5.9	0.0	17	24	0.3
<b>GB</b>	4.5	<b>86.4</b>	9.1	0.0	0.0	22	31	0.003*
<b>IR</b>	18.2	36.4	<b>45.5</b>	0.0	0.0	22	31	0.37
<b>PG</b>	0.0	0.0	66.7	<b>33.3</b>	0.0	6	8	0.22
<b>RDP</b>	0.0	0.0	0.0	0.0	<b>100</b>	5	7	0.003*
<i>Mean</i>					61.3			
<b>Core (QDA)</b>								
<b>PSR</b>	<b>82.4</b>	11.8	0.0	5.9	0.0	17	24	0.003*
<b>GB</b>	4.5	<b>68.2</b>	22.7	4.5	0.0	22	31	0.003*
<b>IR</b>	0.0	18.2	<b>77.3</b>	4.5	0.0	22	31	0.003*
<b>PG</b>	0.0	33.3	0.0	<b>66.7</b>	0.0	6	8	0.03*
<b>RDP</b>	0.0	0.0	0.0	0.0	<b>100</b>	5	7	0.003*
<i>Mean</i>					78.9			
<b>Edge + Shape (LDA)</b>								

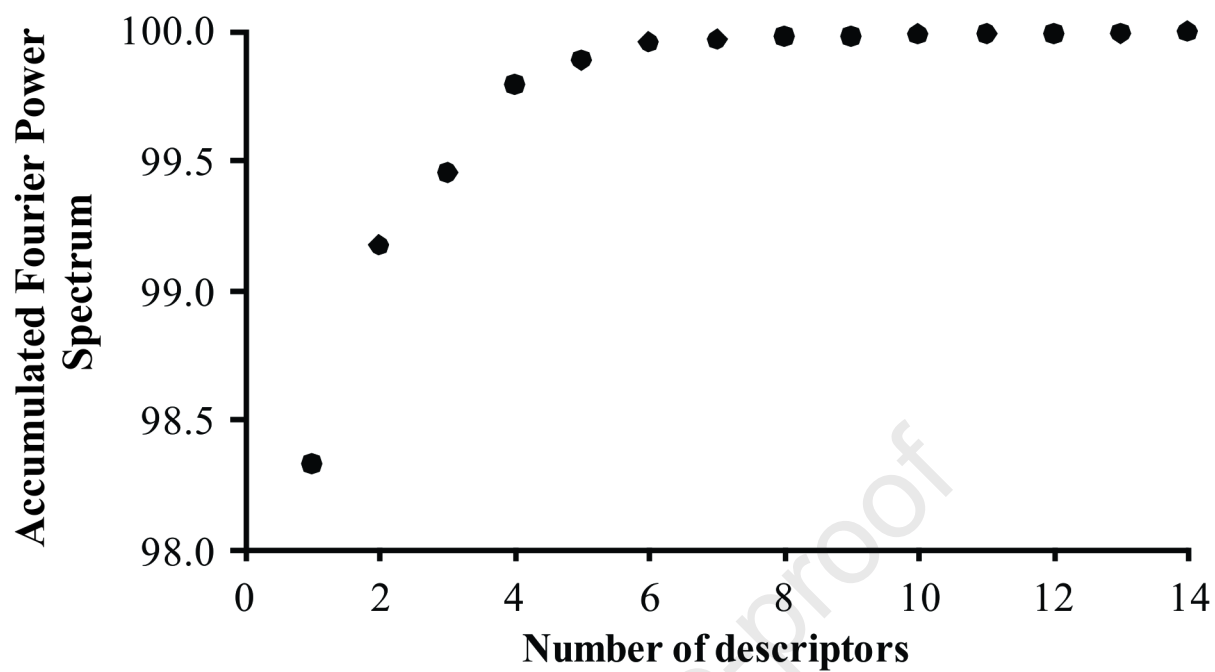
<b>PSR</b>	<b>52.9</b>	11.8	29.4	5.9	0.0	17	24	0.09
<b>GB</b>	14.3	<b>66.7</b>	14.3	4.8	0.0	22	31	0.02*
<b>IR</b>	13.6	27.3	<b>54.5</b>	4.5	0.0	22	31	0.14
<b>PG</b>	33.3	16.7	33.3	<b>16.7</b>	0.0	6	8	0.5
<b>RDP</b>	0.0	0.0	0.0	0.0	<b>100</b>	5	7	0.003*
<i>Mean</i>					58.2			

780

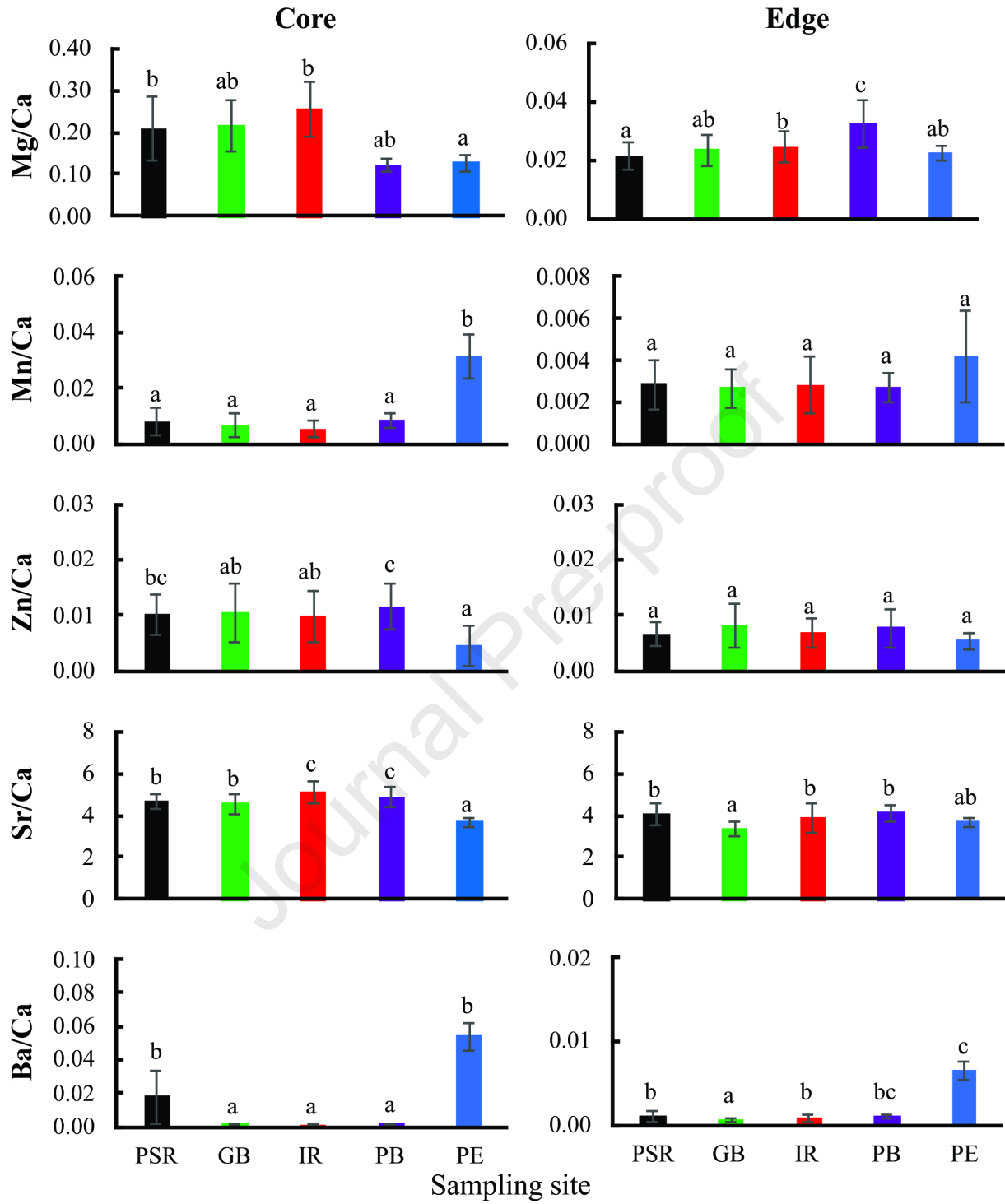
781

782









Spatial segregation in young and adult stages of *Genidens barbatus* was studied.

Otolith microchemistry and shape are potential tools for stock identification.

Results suggest the presence of different management units.

High percentages of classification suggest low connectivity between some populations.

The populations should be managed as separate groups.

Journal Pre-proof

**Declaration of interests**

The authors declare that they have no known competing financial interests or personal relationships that could have appeared to influence the work reported in this paper.

The authors declare the following financial interests/personal relationships which may be considered as potential competing interests:

We have no known competing financial interests or personal relationships that could have appeared to influence the work reported in this paper.

Journal Pre-proof